ELSEVIER

Journal of Biomechanics 35 (2002) 537–542

JOURNAL OF BIOMECHANICS

www.elsevier.com/locate/jbiomech
www.JBiomech.com

Short communication

Accelerometer and rate gyroscope measurement of kinematics: an inexpensive alternative to optical motion analysis systems

Ruth E. Mayagoitia[a,*], Anand V. Nene[b], Peter H. Veltink[c]

[a] *Sport, Health and Exercise, Staffordshire University, Leek Road, Stoke on Trent ST4 2DF, UK*
[b] *Roessingh Research and Development, Roessingh Rehabilitation Institute, Enschede, The Netherlands*
[c] *Biomedical Technology Institute, University of Twente, Enschede, The Netherlands*

Accepted 28 November 2001

Abstract

A general-purpose system to obtain the kinematics of gait in the sagittal plane based on body-mounted sensors was developed. It consisted of four uniaxial seismic accelerometers and one rate gyroscope per body segment. Tests were done with 10 young healthy volunteers, walking at five different speeds on a treadmill. In order to study the system's accuracy, measurements were made with an optic, passive-marker system and the body-mounted system, simultaneously. In all the comparison cases, the curves obtained from the two systems were very close, showing root mean square errors representing <7% full range in 75% of the cases (overall mean 6.64%, standard deviation 4.13%) and high coefficients of multiple correlation in 100% of cases (overall mean 0.9812, standard deviation 0.02). Calibration of the body-mounted system is done against gravity. The body-mounted sensors do not hinder natural movement. The calculation algorithms are computationally demanding and only are applicable off-line. The body-mounted sensors are accurate, inexpensive and portable and allow long-term recordings in clinical, sport and ergonomics settings. © 2002 Elsevier Science Ltd. All rights reserved.

Keywords: Accelerometer; Gyroscope; Gait kinematics; Portable gait analysis; Knee moment

1. Introduction

Optical motion analysis systems are often used in the study of human movement. However, these systems are expensive, only allow measurements in a restricted volume, and the markers are easily obscured from vision resulting in incomplete data. More recently, body-mounted sensors have also been used to obtain kinematic values (Bussmann et al., 1995; Bogert van den et al., 1996; Dai et al., 1996; Luinge et al., 1999; Tong and Granat, 1999; Veltink et al., 1996; Veltink, 1999). A fully portable system can be obtained if a portable data logger is used to gather the data from body-mounted sensors.

The system presented in this paper is general-purpose, combining accelerometers and rate gyroscopes, able to deliver the following kinematic parameters in the sagittal plane: shank angle, thigh angle, knee angle, shank angular velocity, thigh angular velocity, knee linear acceleration, shank angular acceleration and thigh angular acceleration. To verify the accuracy of the body-mounted sensor system, optical data were gathered simultaneously using a Vicon® System. Only the parameters of shank angle, shank angular velocity, knee linear acceleration and shank angular acceleration are presented in this paper as representative examples.

2. Materials and methods

2.1. Model description

In the two-dimensional (sagittal plane) model, the shank and foot were considered as a single segment referred to as shank. Shank and thigh were represented by two rigid segments k and $k+1$ connected by a simple hinge knee joint (Fig. 1).

*Corresponding author. Tel.: +44-1782-294041; fax: +44-1782-294321.
E-mail address: rem2@staffs.ac.uk (R.E. Mayagoitia).

0021-9290/02/$ - see front matter
PII: S0021-9290(01)00231-7

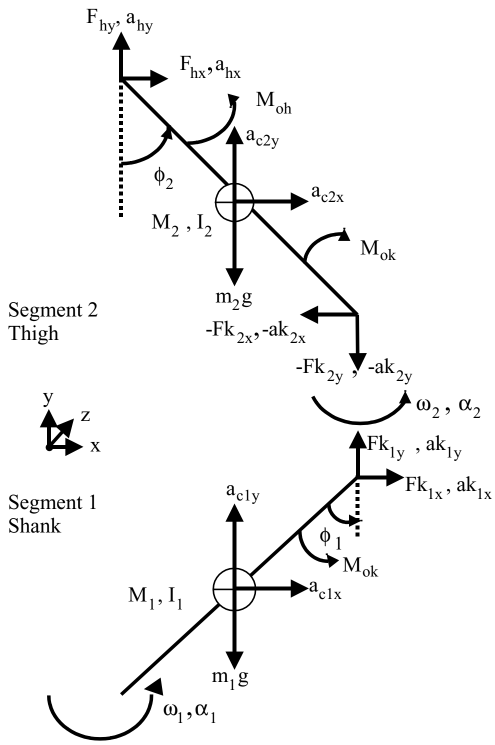

Fig. 1. Free body diagram of the thigh and shank segments during swing.

2.2. Accelerometer signals

2.2.1. Calculation of linear acceleration

The accelerometer signal $\vec{s}_{k,i}$ at any point i of a rigid body k can be expressed as a vector $\vec{x} = (\vec{x}_1, \vec{x}_2, \vec{x}_3)^{\mathrm{T}}$ on the basis of three independent signal vectors $\vec{s}_{k1}, \vec{s}_{k2}, \vec{s}_{k3}$ at positions $\vec{r}_{k1}, \vec{r}_{k2}, \vec{r}_{k3}$ (Veltink and Boom, 1996)

$$\vec{s}_{ki} = \sum_{j=1}^{3} \vec{x}_j \vec{s}_{kj}. \tag{1}$$

The coordinates of vector $\vec{x}$ can be estimated by application of Cramer's Rule. The body-fixed accelerations $\vec{a}^{\mathrm{t}}_{k0}$ and $\vec{a}^{\mathrm{r}}_{k0}$ measured by tangentially and radially oriented accelerometers at the reference point 0 of the body-fixed frame can be represented by

$$\vec{s}^{\,\mathrm{t}}_{k0} = \frac{\vec{r}_{k2}\vec{s}^{\,\mathrm{t}}_{k1} - \vec{r}_{k1}\vec{s}^{\,\mathrm{t}}_{k2}}{\vec{r}_{k2} - \vec{r}_{k1}}, \quad s^{\mathrm{t}}_{k0} = g \sin \varphi_k + a^{\mathrm{t}}_0, \tag{2}$$

$$\vec{s}^{\,\mathrm{r}}_{k0} = \frac{\vec{r}_{k2}\vec{s}^{\,\mathrm{r}}_{k1} - \vec{r}_{k1}\vec{s}^{\,\mathrm{r}}_{k2}}{\vec{r}_{k2} - \vec{r}_{k1}}, \quad s^{\mathrm{r}}_{k0} = g \cos \varphi_k + a^{\mathrm{r}}_0. \tag{3}$$

If the absolute segment angle φ_k is known, it is possible to determine the linear acceleration components a^{t}_0 and a^{r}_0 at this reference point (Willemsen et al., 1991). Eq. (2) is used below to obtain the linear acceleration of the knee.

2.2.2. Calculation of angular acceleration

Two accelerometers tangentially mounted on a rigid body k at point i and $i+1$ measure the tangential acceleration components $\vec{s}^{\,\mathrm{t}}_{k,i+1}$ and $\vec{s}^{\,\mathrm{t}}_{k,i}$. Since g and $\vec{s}^{\,\mathrm{t}}_{k,0}$ are independent of the position along the segment, the quantity $(\vec{s}^{\,\mathrm{t}}_{k,i+1} - \vec{s}^{\,\mathrm{t}}_{k,i})$ is related directly to the angular acceleration:

$$\ddot{\vec{\varphi}}_k = \frac{\vec{s}^{\,\mathrm{t}}_{k,i+1} - \vec{s}^{\,\mathrm{t}}_{k,i}}{\vec{r}_{k,i+1} - \vec{r}_{k,i}}. \tag{4}$$

2.3. Gyroscope signals

2.3.1. Calculation of angular velocity

The angular velocity is measured by a rate gyroscope through the Coriolis force and can be found directly as

$$\vec{\omega}_{\mathrm{gy}}. \tag{5}$$

2.3.2. Calculation of angles

In general, the orientation angle derived from the angular velocity $\vec{\omega}_{\mathrm{gy}}$ measured by a rate gyroscope is given by (Bortz, 1971)

$$\vec{\varphi}_k = \int_t (\vec{\omega}_{\mathrm{gy}} \cdot A + \vec{\omega}_{\mathrm{off}})\,\mathrm{d}t + \vec{\varphi}_{\mathrm{off}}, \tag{6}$$

where $\vec{\omega}_{\mathrm{gy}}$ is the gyroscope output signal, A the proportionality factor, $\vec{\omega}_{\mathrm{off}}$ the angular velocity offset, and $\vec{\varphi}_{\mathrm{off}}$ the initial integration offset ($t = 0$).

The reference angles (integration offset needed by the rate gyroscope) can be obtained from two accelerometers mounted perpendicular to each other at position i on body segment k (Fig. 2) under static conditions with

$$\varphi_{\mathrm{off}} = \arctan \frac{\vec{s}^{\,\mathrm{t}}_{ki}}{\vec{s}^{\,\mathrm{r}}_{ki}}. \tag{7}$$

2.4. Experimental instrumentation

Four pairs of uniaxial accelerometers (IC Sensors 3021-005-P) were mounted on two aluminum strips, 30 cm long and 2 cm wide. The accelerometers measured the tangential and radial accelerations at points i and $i+1$ of each segment (Fig. 2). A gyroscope (Murata ENC-05EB) was attached to the midpoint of each aluminum strip to measure the angular velocity. Data were recorded at 100 Hz.

Calibration recordings were made before and after data collection of each subject. First the strips were placed in line with gravity for two recordings when the radial accelerometers registered $+1g$ and $-1g$. Then the strips were placed perpendicular to gravity, to measure $+1g$ and $-1g$ in the tangetial accelerometers. Dynamic calibrations were made for the gyroscopes putting the sensors through motions of 90° and 180° in a known

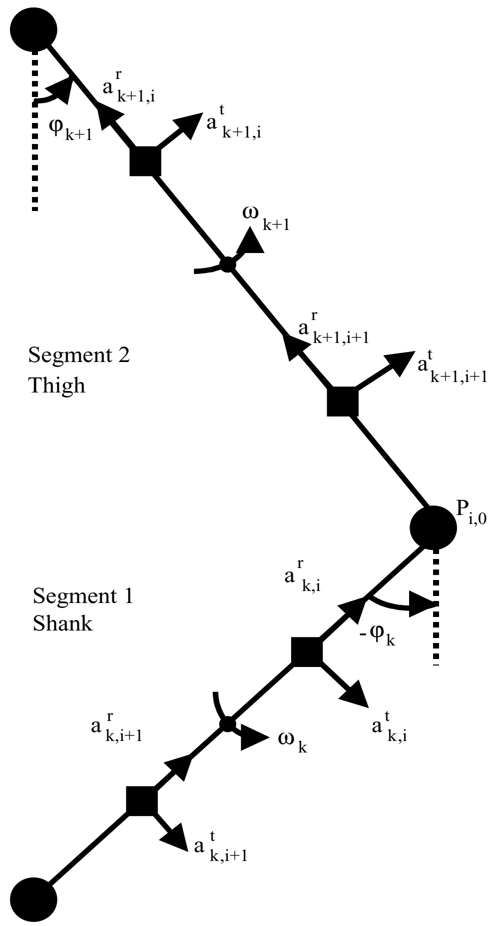

Fig. 2. Accelerometer and rate gyroscope placement on the lower limb.

time. The alignments were assisted by a carpenter's square and a bubble level. For further details on accelerometer calibration, see Veltink et al. (1998).

2.5. Test protocol

Subjects were 10 normal males aged between 23 and 27 years, who had given informed consent. The volunteers performed ten 10 s or 12 s treadmill walking trials consisting of two repetitions at five speeds (very slow = 1.4 km/h, slow = 2.1 km/h, average = 2.7 km/h, fast = 3.6 km/h and very fast = 4.6 km/h) wearing their usual shoes. In addition, two trials of quiet standing before and after each session were recorded.

The aluminum strip with the sensors was placed on the frontal, medial aspect of the shank and thigh of the subject and attached snuggly with wide, elasticized velcro® straps. It was expected that vibration of the metal strip during walking would be minimal and that direct impact of the sensors would be very remote.

Data from the body-mounted system and from a Vicon® motion-measurement system were recorded simultaneously. Reflective markers were placed over the left lateral maleolus, lateral condyle and greater trochanter. The distances between the sensors and the proximal joint marker were measured with a measuring tape. The markers were tracked at 50 Hz.

2.6. Data analysis

Matlab was used for all signal processing. A sixth-order Butterworth low-pass filter with a cut-off frequency of 3 Hz was used to remove noise from all the raw data. Only the sagittal plane components of the recorded marker positions were used. The coordinates of ankle, knee and hip were used to find the displacement of the knee joint and the angular displacement of the shank. By numerical differentiation, the respective velocities were found. A second differentiation yielded the accelerations. The sensor data were decimated to 50 Hz to make the data directly comparable.

For the comparison between the sensor and Vicon® results, the root of the mean of the squared differences (Eq. (8)) was used to compare the closeness in amplitude. Vicon® results were used as reference

$$\mathrm{RMS} = \sqrt{\frac{1}{T}\sum\nolimits_{i=1}^{T}(\varphi_{k\mathrm{r}}(i) - \varphi_k(i))^2}. \tag{8}$$

The subscript r indicates a reference measure. The angle measurement φ_k is used as an example.

A percent error was calculated as the ratio between the RMS error to the average peak-to-peak amplitude of the marker data (Table 1).

The coefficient of multiple correlation (Kadaba et al., 1989) was used to look at the closeness in the shape of the two signals. In this case, the mean of the two signals being compared is used as reference

$$\mathrm{CMC} = \sqrt{1 - \frac{\sum_{j=1}^{N}\sum_{i=1}^{T}(Y_{jt} - \bar{Y}_t)^2/T(N-1)}{\sum_{j=1}^{N}\sum_{i=1}^{T}(Y_{jt} - \bar{Y})^2/(NT-1)}}, \tag{9}$$

where T is the number of samples and N is 2, the number of compared signals.

3. Results

3.1. Measurement system verification

The number of cases (out of 20) in each comparison is indicated in Table 2, together with the RMS and CMC results. Missing cases are due to data lost to file archiving problems or to one or more of the markers being lost from vision. Fig. 3 shows examples of graphs of the four comparisons.

In three of the four comparisons, the RMS errors are <7% of the full range of the measurements and the found CMC are above 0.98. However, for the linear acceleration of the knee (comparison number 3), the

Table 1
Percent errors of the kinematic measurements. Ratio of RMS error to average peak to peak values obtained from our own optical marker results

	1. Shank angle Gyroscopes vs. Vicon RMS (rad)	2. Shank angular velocity Gyroscopes vs. Vicon RMS (rad/s)	3. Knee linear acceleration Accelerometers vs. Vicon RMS (m/s/s)	4. Shank angular acceleleration Accelerometers vs. Vicon RMS (rad/s/s)
Very slow				
Mean	0.0478	0.1638	0.5848	1.5801
Ref	0.92	4.2	4.1	33.0
% error	5.2	3.9	14.2	4.8
Slow				
Mean	0.0379	0.2153	0.7860	2.3168
Ref	1.01	5.2	6.0	45.2
% error	3.7	4.2	13.2	5.1
Intermediate				
Mean	0.0295	0.2721	0.9613	2.9007
Ref	1.09	6.1	8.4	55.6
% error	2.7	4.5	11.5	5.2
Fast				
Mean	0.0333	0.3522	1.4393	3.8329
Ref	1.19	7.0	11.2	68.0
% error	2.8	5.0	12.9	5.6
Very fast				
Mean	0.0238	0.4338	2.1609	5.3366
Ref	1.26	8.3	14.6	84.4
% error	1.9	5.2	14.8	6.3

Percentage error of RMS (mean) to Vicon full range (ref) (Ref = peak-to-peak values averaged).

Table 2
Results of comparing kinematic measurements obtained by body-mounted sensors and optical markers

	(1) Shank angle Gyroscopes vs. Vicon		(2) Shank angular velocity Gyroscopes vs. Vicon		(3) Knee linear acceleration Accelerometers vs. Vicon		(4) Shank angular acceleration Accelerometers vs. Vicon	
	RMS (rad)	CMC	RMS (rad/s)	CMC	RMS (m/s/s)	CMC	RMS (rad/s/s)	CMC
Very slow								
Mean	0.0478	0.9844	0.1638	0.9949	0.5848	0.9363	1.5801	0.9870
Stdev	0.0496	0.0283	0.0378	0.0017	0.1071	0.0208	0.2746	0.0043
Cases	17		12		14		12	
Slow								
Mean	0.0235	0.9983	0.2153	0.9947	0.7859	0.9499	2.3168	0.9861
Stdev	0.0100	0.0015	0.0521	0.0020	0.2464	0.0237	0.5430	0.0068
Cases	17		15		17		15	
Intermediate								
Mean	0.0295	0.9961	0.2721	0.9945	0.9613	0.9616	2.9007	0.9885
Stdev	0.0341	0.0116	0.0481	0.0013	0.2683	0.0181	0.5600	0.0020
Cases	17		16		17		16	
Fast								
Mean	0.0333	0.9947	0.3522	0.9935	1.4393	0.9540	3.8329	0.9880
Stdev	0.0468	0.0172	0.0563	0.0017	0.3380	0.0174	0.4630	0.0018
Cases	16		15		18		15	
Very fast								
Mean	0.0238	0.9990	0.4338	0.9930	2.1609	0.9438	5.3366	0.9862
Stdev	0.0056	0.0005	0.0650	0.0019	0.5874	0.0223	0.6585	0.0033
Cases	16		16		17		16	

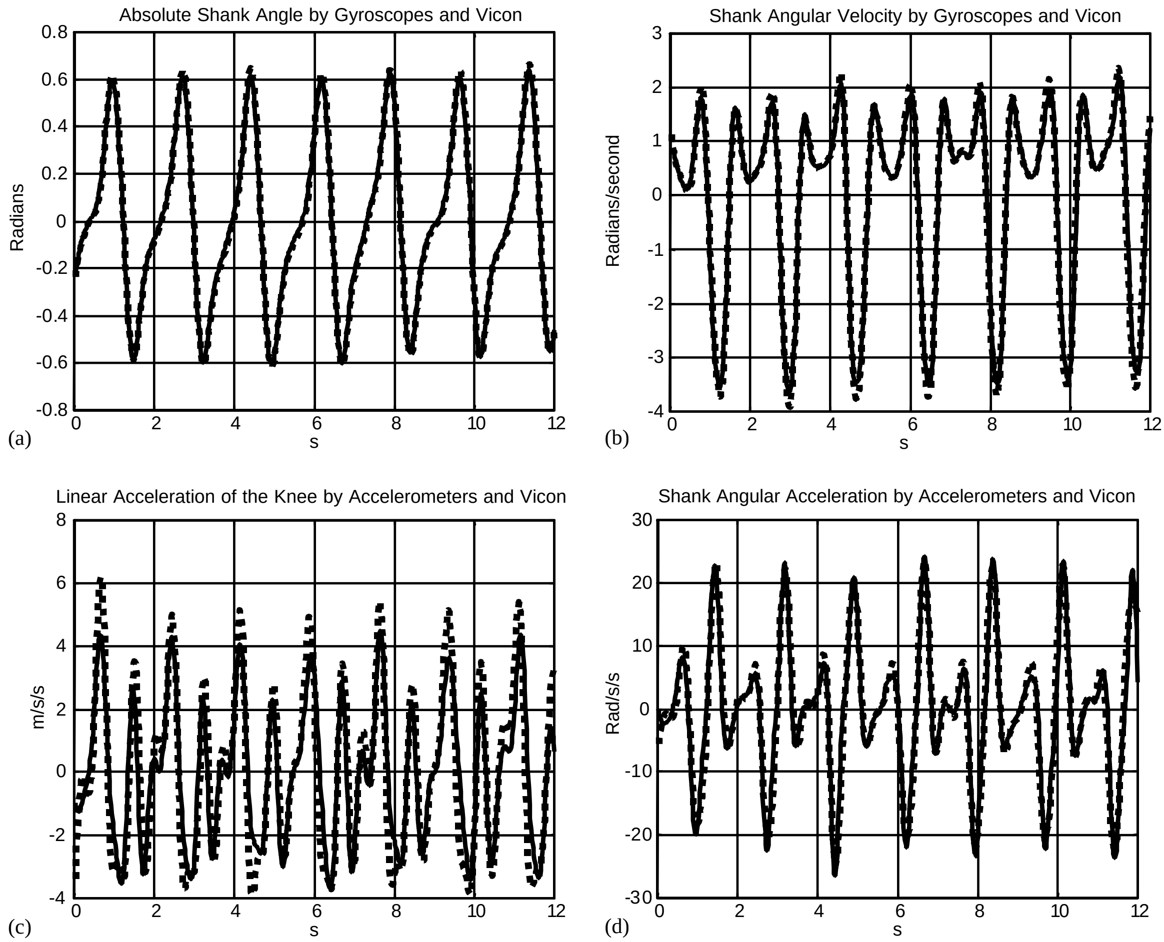

Fig. 3. Representative graphs to illustrate comparisons a–d; subject number 7, intermediate velocity. Vicon—solid line. Sensors—dashed line.

errors are between 11% and 15% and CMCs drop to 0.93. The algorithm to calculate the linear acceleration of the knee from accelerometer data depends on the distance between the proximal tangential accelerometers on thigh and shank and the knee joint. Slippage of the strip on which the sensors were mounted would give a rise to a change in the actual distance between the sensors, and this could account for the small, over estimation. The distance between the sensors and the knee was only measured at the beginning of the session.

4. Discussion

4.1. Accuracy of kinematic measurements

The body-mounted sensors give results that are very close to those of Vicon® presenting small RMS and large CMC values. Errors do increase at the highest speed for the accelerometer data, which for several subjects suffered from deformed peaks, probably due to the sensors being hit or vibrated during heel strike. This should be taken into account when designing future applications involving accelerometers. The rate gyroscopes were not affected in this way.

4.2. Contributions of this study and future work

In this study, a treadmill was used within the vision cube of the Vicon® system in order to record several consecutive steps. There are subjects for whom it would not be safe to use a treadmill. However, the body-mounted sensors combined with a portable data-logger constitute a fully portable system that can be used for as many consecutive steps as desired in almost any environment. The body-mounted sensor system subject of this paper has been applied in a biomechanics study (Nene et al., 1999). A similar system could also be used in sports situations with accelerations comparable to those of walking.

The method for finding kinematics by using body-mounted accelerometers and rate gyroscopes is accurate as compared to a Vicon® system, for different normal subjects and at five different walking speeds. The system based on body-mounted sensors is inexpensive. The metal strip where the sensors are mounted is more cumbersome than the markers but does not alter movement.

Acknowledgements

We are grateful to the STW, Dutch Technology Foundation, for the funding for this project; to Andreas Heyn and Eric Camiro for their valuable assistance.

References

Bogert van den, A.J., Read, L., Nigg, B.M., 1996. A method for inverse dynamic analysis using accelerometry. Journal of Biomechanics 29, 949–954.

Bortz, J.E., 1971. A new mathematical formulation for strapdown inertial navigation. IEEE Transactions on Aerospace and Electronic Systems 7, 61–66.

Bussmann, J.B.J., Veltink, P.H., Koelma, F., van Lummel, R.C., Stam, H.J., 1995. Ambulatory monitoring of mobility-related activities: the initial phase of the development of an activity monitor. European Journal of Physical and Medical Rehabilitation 5, 2–7.

Dai, R., Stein, R.B., Andrews, B.J., James, K.B., Wieler, M., 1996. Application of tilt sensors in functional electrical stimulation. IEEE Transactions on Rehabilitation Engineering 4, 63–72.

Kadaba, M.P., Ramakrishnan, M.E., Gainey, W.J., Gorton, G., Cochran, G.V.B., 1989. Reproducibility of kinematic, kinetic, and electromyographic data in normal adult gait. Journal of Orthopedic Research 7, 849–860.

Luinge, H.J., Veltink, P.H., Baten, C.T.M., 1999. Estimating orientation with gyroscopes and accelerometers. Technology and Health Care 7, 455–459.

Nene, A., Mayagoitia, R.E., Veltink, P.H., 1999. Assessment of rectus femoris function during initial swing phase. Gait and Posture 9, 1–9.

Tong, K., Granat, M.H., 1999. A practical gait analysis system using gyroscopes. Medical Engineering and Physics 21, 87–94.

Veltink, P.H., 1999. Sensory feedback in artificial control of human mobility. Technology and Health Care 7, 383–391.

Veltink, P.H., Boom, H.B.K., 1996. 3D movement analysis using accelerometry—theoretical concepts. In: Pedotti, A., Ferrarin, M., Quintern, J., Riener, R. (Eds.), Neuroprosthetics—From Basic Research to Clinical Applications. Springer, Berlin, pp. 317–326.

Veltink, P.H., Bussmann, H.B.J., Vries de, W., Martens, W.L.J., Lummel van, R.C., 1996. Detection of static and dynamic activities using uniaxial accelerometers. IEEE Transactions on Rehabilitation Engineering 4, 375–385.

Veltink, P.H., Lötters, J.C., Schipper, J., Olthuis, W., Bergveld, P., 1998. Procedure for in-use calibration of triaxial accelerometers in medical applications. Sensors and Actuators A 68, 221–228.

Willemsen, A.T.M., Frigo, C., Boom, H.B.K., 1991. Lower extremity angle measurement with accelerometers—error and sensitivity analysis. IEEE Transactions on Biomedical Engineering 12, 1186–1193.